

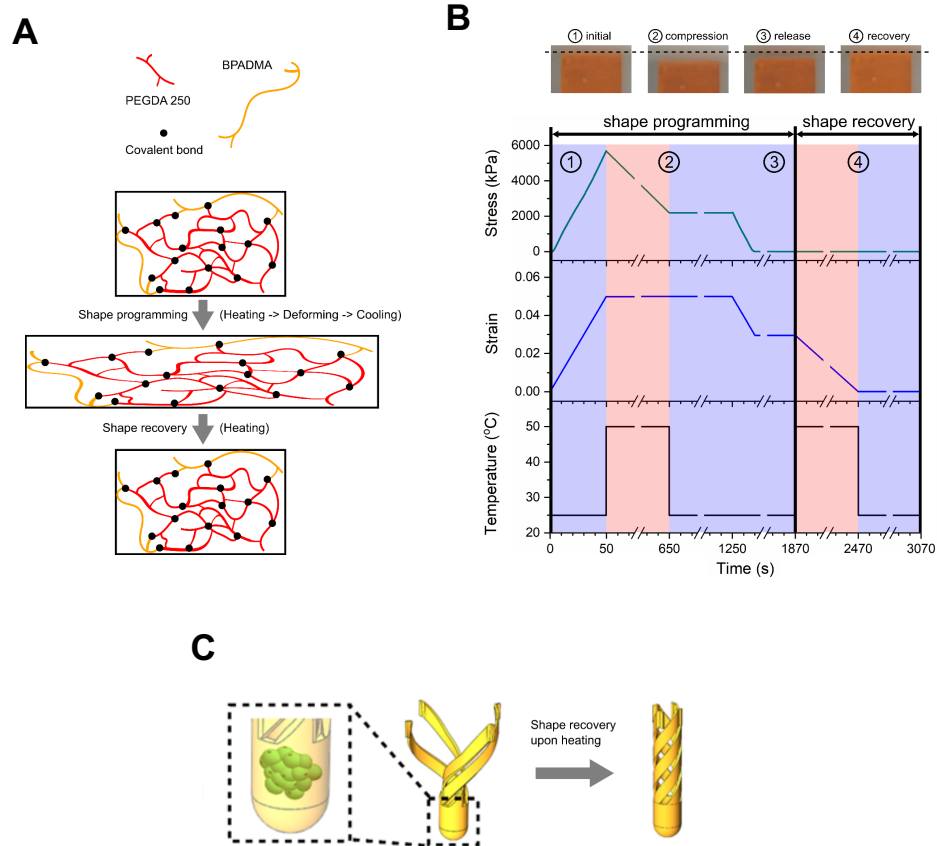
**iScience, Volume 23**

**Supplemental Information**

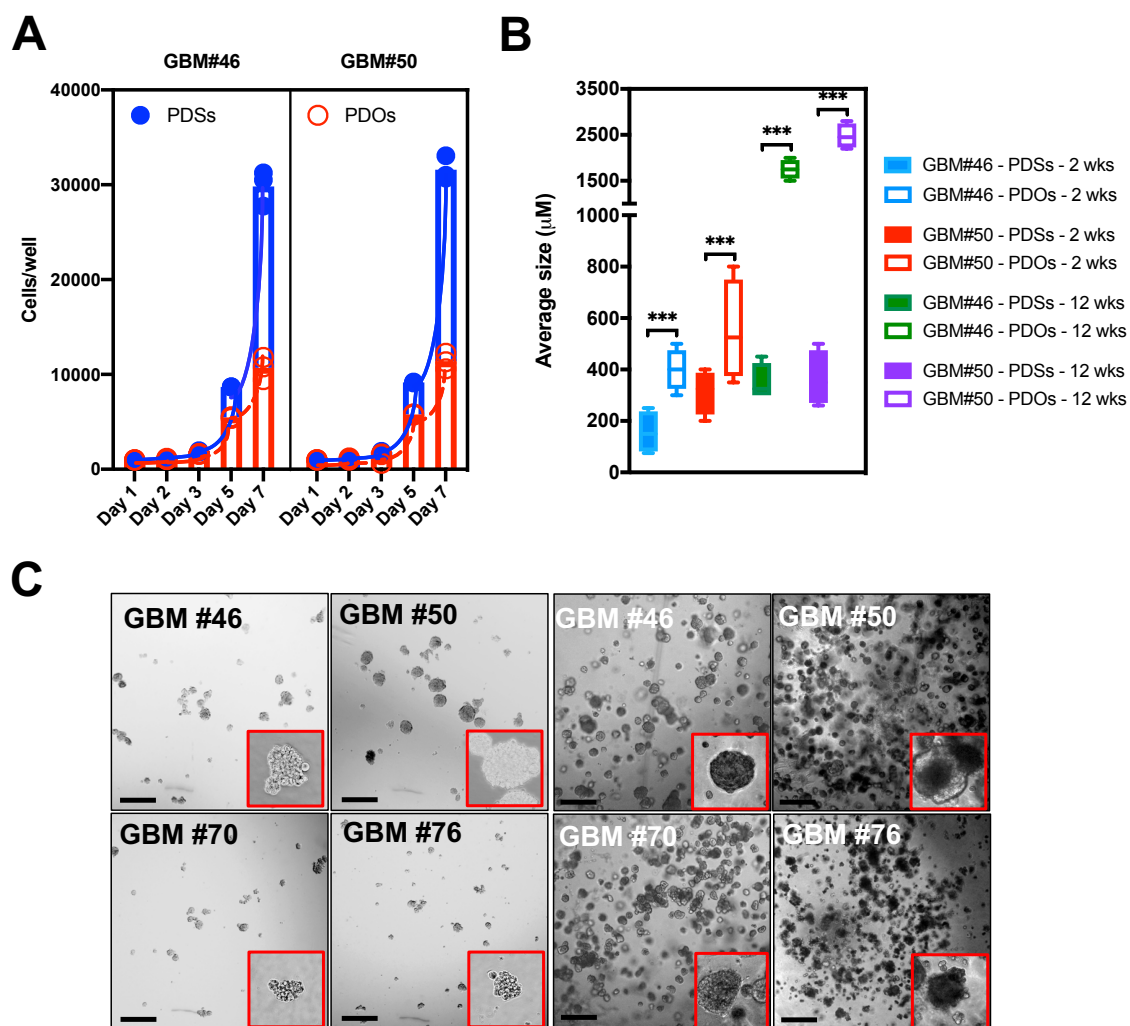
**Rapid Processing and Drug Evaluation  
in Glioblastoma Patient-Derived  
Organoid Models with 4D Bioprinted Arrays**

**Michelle Chadwick, Chen Yang, Liqiong Liu, Christian Moya Gamboa, Kelly Jara, Howon Lee, and Hatem E. Sabaawy**

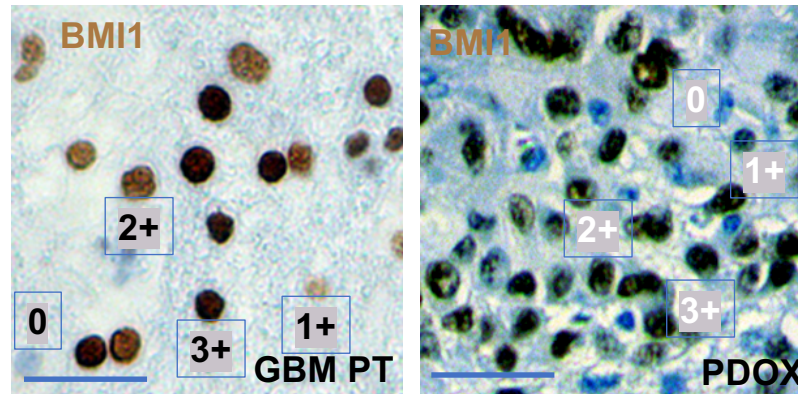
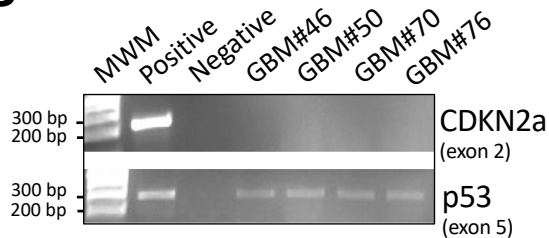
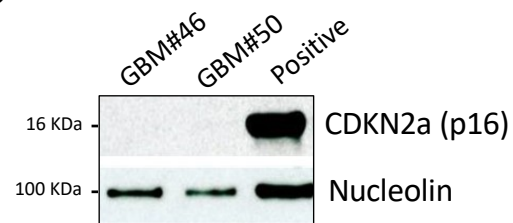
SUPPLEMENTAL DATA:



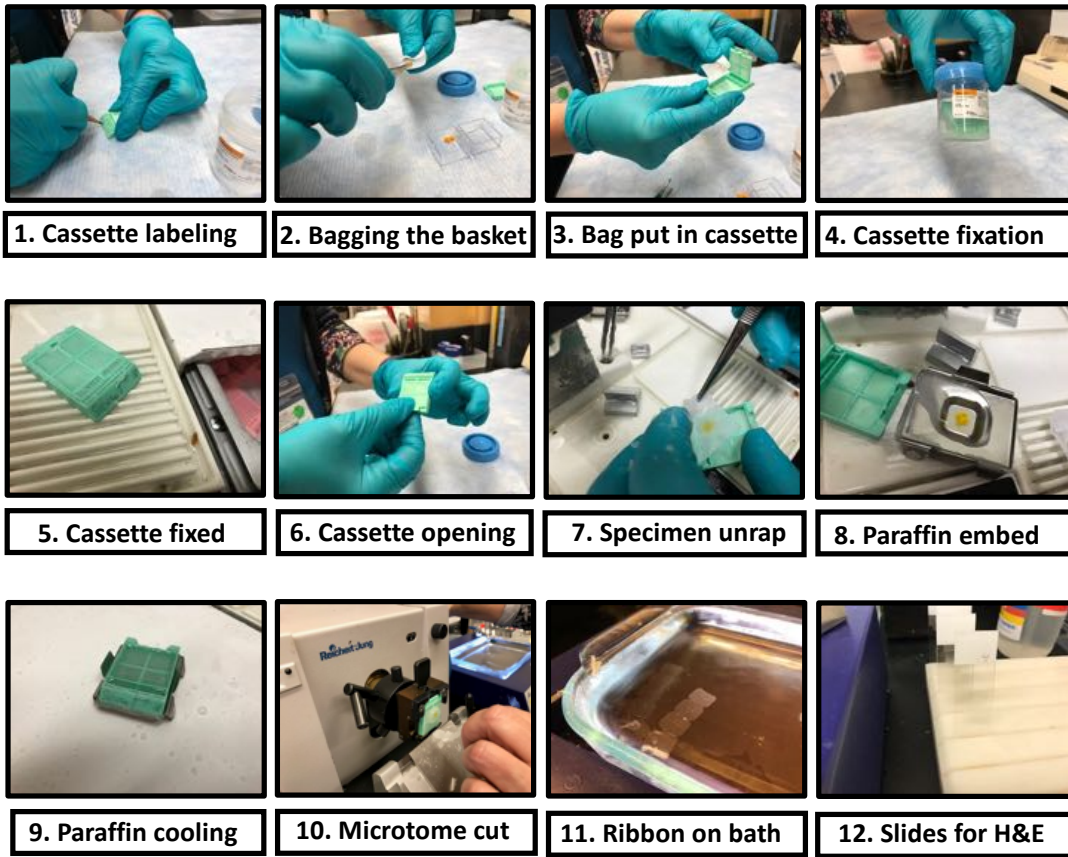
**Figure S1. Shape memory effect of the shape memory polymer utilized to generate the 4D printed cell-culture insert arrays. Related to Figure 1.** (A) A schematic showing the SMP materials PEGDA 250 and BPADMA used to manufacture the cell-culture insert array by forming cross-linked polymeric network. These SMP interconnect through covalent bonds created during photopolymerization. During shape programming, the temperature was first raised to mobilize polymer chains for deforming the polymer network, while covalent bonds remain unchanged. Since mobility of polymer chains decreases at low temperature, the deformed shape can be temporarily fixed. When heated, the polymer chains become mobilized again, restoring its original thermodynamic- favored shape without any external stress. (B) A diagram showing the thermodynamic features of the SMP. A beam was compressed by 5% at 25°C. While maintaining the strain, the beam was heated to 50°C and then cooled down to 25°C again. Note that the required stress to maintain the compressive strain was significantly reduced due to fixing of the deformed shape. After removal of the mechanical loading, the deformed strain was retained at 3%. Upon heating back to 50°C, the original height of the beam could be completely recovered. (C) A diagram demonstrating the design advantage of the array with a lower cell compartment protecting the biological materials from external stresses. The lower cell compartment of a representative well from the cell-culture insert array harboring inside the biological material (e.g. PDOs), while the large deformation enabling the shape transformation to occur in the upper helical bridges. When heating is applied, PDO cells have already undergone fixation with formaldehyde. Therefore, no distortion due to external stress or heating was noticeable when using the arrays.



**Figure S2. Features of GBM-PDO cells. Related to Figure 2.** (A) Cell counts per well during the first 7 days of GBM-PDS and -PDO cultures. PDSs were rapidly proliferating between days 3-7 much faster than PDOs. After day 7, GBM-PDOs continued to grow and were significantly bigger at day 14 and up to 12 weeks in culture. (B) Average size of GBM-PDSs and -PDOs based on microscopic and image J analysis. (C) Bright field images of 3D cultured GBM-PDSs (left) and -PDOs (right) after 12 weeks of culture. Comparison between PDSs vs PDOs in (A and B) are represented as mean  $\pm$  S.D. of 4 replicates and significance was determined by one-way ANOVA (\*\*\*)  $p < 0.001$ ).

**A****B****C**

**Figure S3. BMI1, CDKN2a and p53 levels assessment in GBM patients and models. Related to Figures 4 and 5.** (A) Representative IHC images of BMI1 expression in the originating GBM#46 and their derived mouse PDOX. Scoring of cells with representative BMI1 level (0-3+) is demonstrated next to each corresponding representative cell. Images were quantified for the amount of BMI1 positive staining, as well as for intensity of the staining. H scores were calculated as  $(\% \text{ at } 0) * 0 + (\% \text{ at } 1+) * 1 + (\% \text{ at } 2+) * 2 + (\% \text{ at } 3+) * 3 = \text{Range } 0 - 300$  based on analyses of at least 10 fields per slide averaged by two qualified examiners. H scores were  $148 \pm 12$  for GBM#46 and averaged  $132 \pm 22$  from 4 PDOXs derived from GBM#46. (B) PCR amplification of genomic DNA from GBM#46, GBM#50, GBM#70 and GBM#76 revealed that exon 2 of the CDKN2A locus, which is shared between both p16<sup>INK4a</sup> and p14<sup>ARF</sup>, failed to amplify when compared to genomic DNA from HEK293T cells (positive), while amplification of PCR products corresponding to exon 5 of TP53 (p53, exon 5) could be detected from these GBMs. MWM, molecular weight marker. These data, together with the Glioseq data, suggested that cells from these four GBMs have homozygous CDKN2a losses. (C) The genomic data of CDKN2a homozygous losses were confirmed at the protein level from the GBMs with available tissues when compared to HEK293T cells, there was no detectable CDKN2a (p16) expression at the expected size (16 KDa), even after over-exposure of lysates from the positive control. Nucleolin levels were used as nuclear/loading controls with an observed band size of 100 KDa. Data represent three independent experiments.



## Images of histological processing steps

Figure S4. Histological processing steps of 4D cell-culture insert arrays. Related to Figures 1 and 4. Demonstration of the twelve steps used in the manual histological processing of the biospecimen in the cell-culture insert arrays. Automatic histological processing has also been examined and SMP cell-culture insert arrays were compatible with the automated processing.

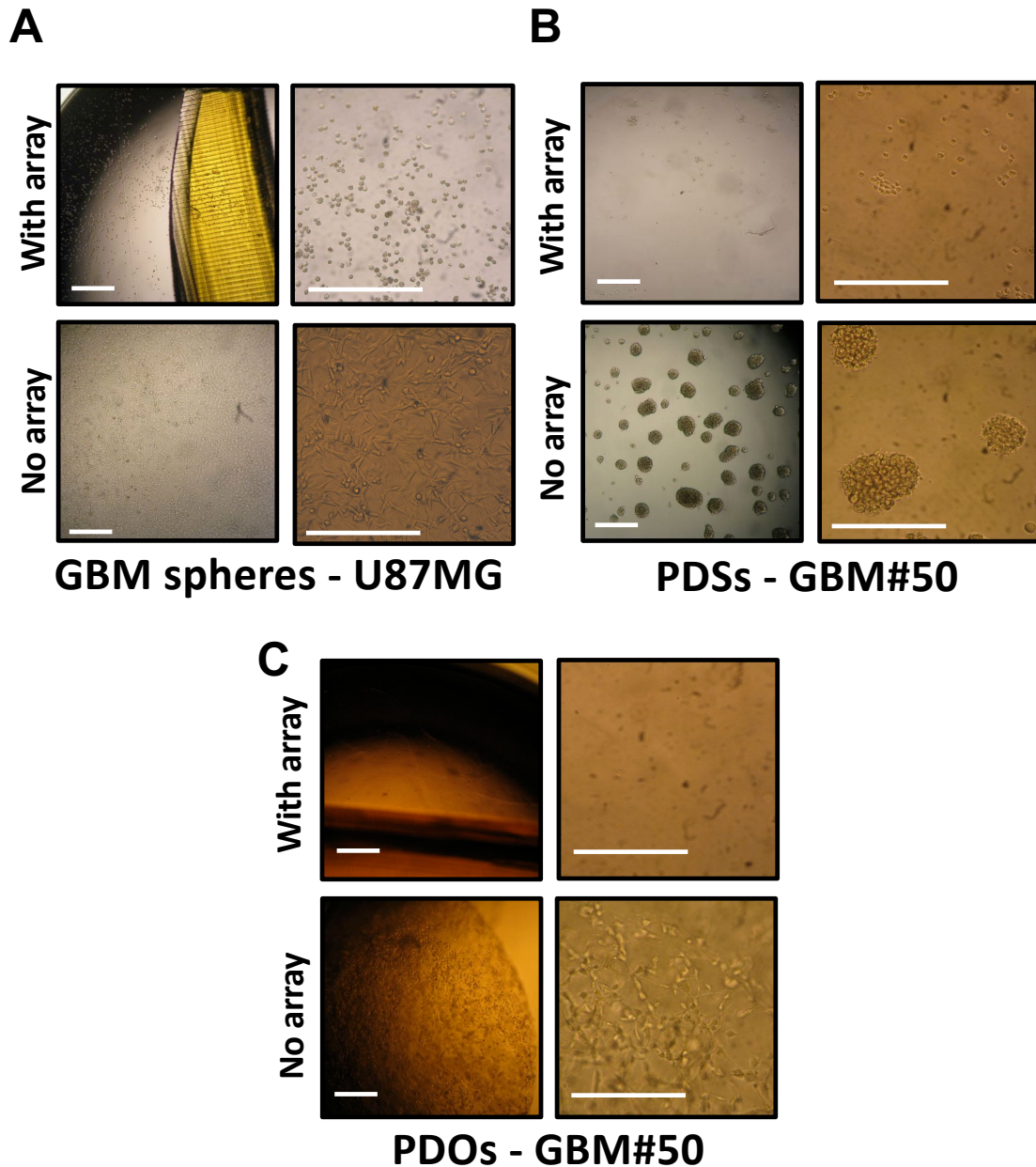


Figure S5. Biocompatibility of the 4D printed cell-culture insert arrays. Related to Figures 1 and 4. (A) Examination of GBM U87MG cells cultured in sphere culture conditions and GBM#50 PDS and PDO cultures with or without the 4D SMP arrays. (B) Images of 3D cultured GBM#50 PDSs with or without the 4D SMP arrays. (C) Images of 3D cultured GBM#50 PDOs with or without the 4D SMP arrays. Scale bars in (A-C) are 100  $\mu$ m.

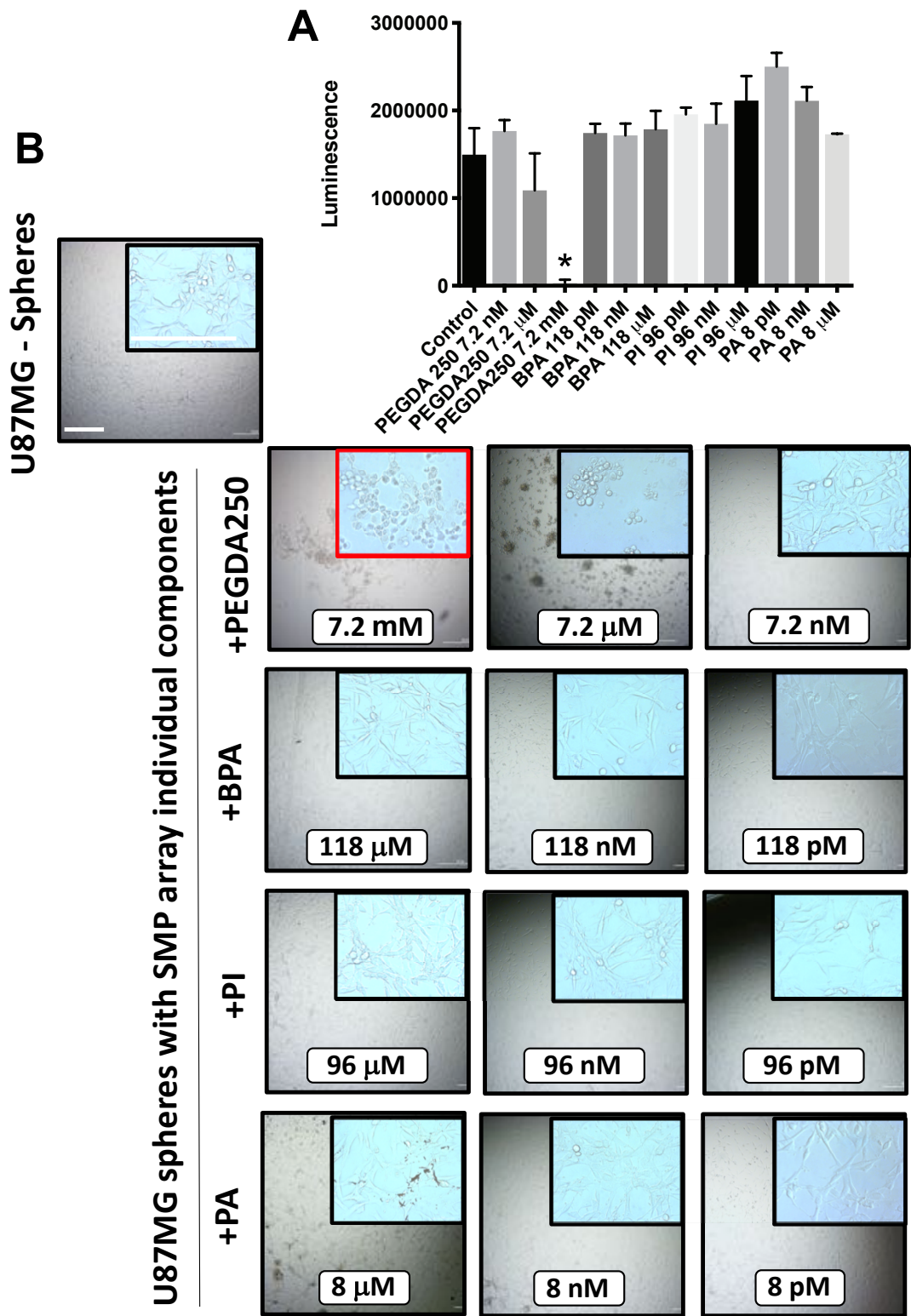
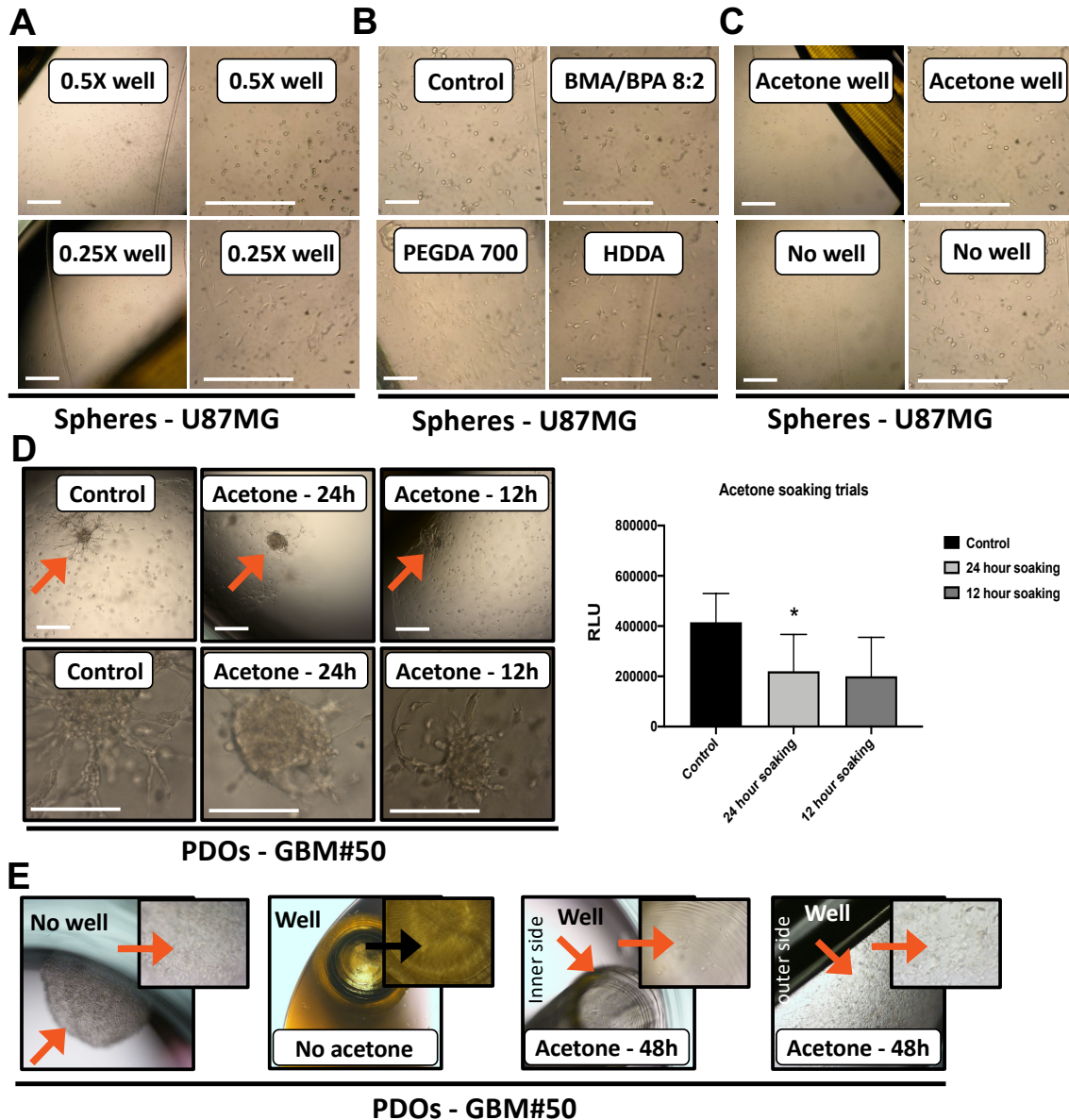


Figure S6. Components of additive manufacturing for generating the 4D printed cell-culture insert arrays are tested for effects on GBM sphere formation. Related to Figures 1 and 4. (A) Cell viability of U87MG cells cultured in sphere conditions for one week in the presence of each chemical

component used for the 4D printing and additive manufacturing of the SMP array. Testing for each component was performed over a 2Log concentrations, and displayed at concentrations ranging from mM to pM for each chemical. (B) Representative bright field images of U87MG cells in sphere culture conditions for one week in the presence of individual components of the SMP chemicals at the indicated conc. Insets are higher power (20X) magnification of the 5x images. Luminescence effects of different chemicals are represented as mean  $\pm$  S.D. of three replicates and significance was determined by student t test (\* $p < 0.05$ ). Only PEGDA250 when used at 7.2 mM (1,000 times higher concentration than the 7.2  $\mu$ M concentration used for manufacturing the SMP) induced a significant reduction in cell viability (red inset). Scale bars in control image on the left and all treatment images are 100  $\mu$ m.





**Figure S7. Acetone soaking allowed the use of 4D printed cell-culture insert arrays for GBM sphere and organoid long-term culture. Related to Figures 1 and 4.** (A) PDS culture with individual well components of arrays in 3D sphere culture conditions for one week. (B) Images of sphere culture with selected components of the SMP and 4D printing chemicals that were individually examined at the final concentrations used in the prototype array to define the conditions that allowed normal sphere culture. (C) Images showing that incubation of 4D printed insert array wells in 100% acetone bath after 3D printing allows normal sphere culture. (D) GBM-PDO culture upon soak trials for 12-24 hour in acetone gradually improved 3D cultures. Data are represented as mean  $\pm$  S.D. of four replicates and comparisons between acetone soaking trials and control were assessed by student t test ( $*p < 0.05$ ) and determined that at least 24-hour of acetone bath soaking is required. (E) Incubation of 4D printed cell-culture insert arrays in 100% acetone bath after 3D printing for 5 days was finally determined to allow normal GBM organoid-like culture. Bright field images showing organoid-like growth within the insert array upon soaking in 100% acetone bath for 5

days after 3D printing (red arrows, images showing comparable growth to the no array well control at 48 hours), compared to no organoid growth when an acetone bath was not used (no acetone, black arrow). Panels on the right are higher magnifications of the images on the left in (A, C and E) and panels on the bottom are higher magnifications of the images on the top in (D). Scale bars in (A-D) are 100  $\mu\text{m}$ .

## TRANSPARENT METHODS

### Materials

All chemicals including both liquid oligomers, photoinitiator (PI) and photo absorber (PA) were purchased from Sigma-Aldrich (St. Louis, MO, USA). For 3D printing, poly(ethylene glycol) diacrylate (PEGDA) (Mn250) and Bisphenol A ethoxylate dimethacrylate (BPADMA) (Mn 1700) were used. Phenylbis(2,4,6-trimethylbenzoyl) phosphine as PI and Sudan I as PA were used to initiate polymerization and control UV light penetration, respectively.

### Processing of 4D printed cell-culture insert arrays

4D printing refers to 3D prints with smart materials that is responsive to external stimuli (Yang et al., 2019). Key elements for generating the 4D printed arrays included determining the 3D printability, 3D shapes between which self-transformation occurs (a cell-culture insert array and a histology mega-cassette), PI and PA properties and thermo-stimulus properties. The smart material utilized in this study was a shape memory polymer (SMP), and the high precision 3D printing technique was projection micro-stereolithography (P $\mu$ SL) (Yang et al., 2019; Zheng et al., 2012). SMPs were fixed in a temporarily deformed shape and restored to the original shape upon heating around glass transition temperature ( $T_g$ ) (Yang et al., 2019; Zheng et al., 2012). Mathematical modeling may predict the transition and final state of 4D printed constructs (Ashammakhi et al., 2018). Mathematical modeling was performed to assess the outcome of multiple printing processes and determine the state of printed materials upon applying different stimuli (Lee laboratory, unpublished data). 3D printed cell-culture insert arrays were rinsed four times in fresh ethanol for 30 second each to remove non-crosslinked precursor solution. After air drying, the inserts were rinsed in pentane and post-cured in a UV oven (UVP, 365 nm) for 2 hours. To eliminate toxicity from any residual 3D printing material, the inserts were soaked in an acetone bath for 5 days, rinsed in ethanol and PBS for sterilization and dried overnight at room temperature (RT).

### Operation of 4D printed culture inserts

For operating the culture insert, at RT, an insert in the cassette configuration was first mounted on a custom-built stretcher. The insert was stretched to 96-well plate configuration at RT. After rotation, both the insert and the stretcher were placed in an oven at 50°C for 20 minute and then cooled down to RT to program the stretched shape. The insert was then mounted onto a fixture and a 96-well plate. Cells and culture media were injected into each well using micropipette. After cell culture, the insert was removed from the fixture and heated to 50°C to induce shape recovery to the cassette configuration while maintaining the registry of the cultured cells. In the cassette configuration, the insert was ready for histological processing to obtain the histology of the entire 4D printed culture inserts.

### Quantitative RT-PCR

We performed GBM subtype gene signatures and gene expression profiling using a subset of markers based on TCGA database and signatures associated with tumor histology, grade and defining molecular features (Jin et al., 2017). For Quantitative RT-PCR, total RNA was isolated with the RNeasy kit (Qiagen) and reverse-transcribed into cDNA using the aScript cDNA SuperMix (Quanta Biosciences). Real-time PCR was performed on an Applied Biosystems StepOne Plus cycler using SYBR-green Mastermix (Thermo Scientific). Expression values were normalized to 18S.

### **Patient derived 3D cell culture**

To generate patient-derived 3D cell culture, patient samples were obtained from patients undergoing resection at Robert Wood Johnson University Hospital under an Institutional Review Board approved protocol. GBM tissues were processed mechanically by cutting into small pieces (<1mm) and were incubated in serum-free media (Advanced DMEM F12 (Gibco, REF #12634-010) with primocin (InvivoGen, ant-pm-1), B27 (Gibco, REF #12587-001), EGF (PeproTech, #AF-100-15-100UG) and FGF (PeproTech, #AF-100-18B-500UG) at 20 ng/mL). They were then incubated with Accutase at 37°C for 2-4 minute and passed through a needle to obtain single cell suspension. Cells were plated in the serum-free media on ultra-low attachment plates (Grenier, #655185) and treatments were done in these 96-well plates. PDSs were utilized for clonogenic assays by allowing limiting dilution of GBM cells to form gliospheres, defined as clusters of greater than 50 cells and larger than 50  $\mu\text{m}$  in diameter, for 7 days. Every two days, half of the media were replaced and gliospheres were counted. Single cells from day-7 gliospheres were used in secondary and tertiary gliosphere assays (Mehta et al., 2015), and the sphere forming potentials were determined (Bansal et al., 2016). The organoid forming potential data were similarly determined from day-14 GBM-PDOs. Data were analyzed using ELDA software (<http://bioinf.wehi.edu.au/software/elda/>).

### **Generation, imaging and analysis of 3D GBM-PDOs**

To generate patient-derived organoids, cells grown in serum-free media were mixed at  $10^3$  cells/well of a 96-well plate in 20% media and 80% Matrigel (Corning, REF# 356237). From this initial mix, 10  $\mu\text{L}$  were injected per well of the 4D printed culture inserts using a microinjection p20 pipette. The 4D printed culture inserts were placed at 37°C for one hour. After this hour, 300  $\mu\text{L}$  of organoid media was added per well (Neurobasal media (Gibco, REF #21103-049), B27 (-Vitamin A), sodium pyruvate (Himedia, TCL015-100ML), hydrocortisone (1 mM), EGF and FGF at 20 ng/mL). Media for PDO cultures were partially (~80%) replaced three times per week and 3D cultures were performed between one week to 12 weeks. In some cases, organoid cultures were transferred to bioreactors under similar conditions (Lancaster et al., 2013), and only after 2 weeks of 3D plate cultures to reduce the development of organoid central necrotic cores. These organoids in the bioreactor tended to fuse into larger organoids when cultures were extended for 12 weeks and were not considered for drug testing assays. In an organotypic migration and invasion model, GBM-PDO cell migration from within the matrigel droplets to the plate or culture insert surface and invasion of the surrounding matrigel droplets in three-dimensional matrices were captured with phase contrast using the IncuCyte HDs system. Frames were captured at 4-hour intervals from time 0 to 72 hour from 2 separate regions/well using a x10 objective. Image processing involved fluorescent color-channel separation, data resizing, illumination adjustment and threshold setting and data extraction for each GBM-PDO.

### **Immunofluorescence (IF), WB and IHC**

IF and IHC titration of antibodies and basic conditions were established (Kramer et al., 2013; Patel et al., 2012), and modified to adapt to 3D culture models and for using with the cell-culture insert arrays. Organoid-like cultures within the 96- or 24-well plates without the array or within the 96- or 6-well plates with the array were fixed for 10 minutes at 37°C with 4% paraformaldehyde followed by 3 washes with PBS. For IF, they were permeabilized overnight at 4°C with 0.5% Triton X-100 in PBS followed by 3 washes with PBS. Primary antibody was incubated at RT overnight followed by 3 washes in PBS. Secondary antibody with phalloidin (Life Technologies, REF#

A12380, 1:200) and DAPI (Invitrogen, REF# D1306, 1:200) were incubated overnight at RT followed by 3 washes in PBS. Images were taken on a Nikon A1R Si confocal microscope. For IHC, following fixation, the organoids were taken to pathology where they were processed and embedded in paraffin. They were then sectioned at a thickness of 5  $\mu$ M. They were then stained using the Ventana Discovery XT automated IHC instrument. For phospho S6 assays, PTEN status in GBMs or GBM-PDOs were determined against control PTEN-proficient and -deficient GBM tissues to establish phospho S6 expression detection levels (Baeza et al., 2003). Antibodies were used against these targets: BMI1 (CST, #6964, 1:200), GALC (Santa Cruz Biotechnology, sc-67352, 1:100), GFAP (Cell Signaling Technologies (CST, #3670, 1:200), phospho S6 (CST, #2215, 1:50), NESTIN (Millipore, #MAB5326, 1:50), SOX2 (CST, #23064, 1:400), TLX (Invitrogen, #PA5-40484, 1:100), and TUJ1 (Millipore, #MAB1637, 1:100). Antibodies used for WB were for: p16 (2D9A12) (Santa Cruz Biotechnology, sc-81157, 1:1,000) and Nucleolin (Abcam, #ab22758, 1:1,000).

### **Generation of mouse PDOX**

Mice were anesthetized with 100 mg/kg Ketamine (Henry Schein, NDC 11695-0702-1) and 10 mg/kg Xylazine (Akorn, NDC 59399-110-20) in PBS. The scalp was shaved, and the mouse immobilized within a stereotactic device. An incision was made to expose the bregma. A small hole was created based on the bregma- X: 2.5 mm right and Y: 1.5 mm anterior using a drill. A Hamilton syringe was used to inject  $3-8 \times 10^4$  GBM cells in 4  $\mu$ L over 7.5 minutes at 3.5 mm deep at stereotaxic coordinates of 1 mm posterior to the bregma and +2 mm mediolateral from the midline. The syringe was slowly removed over 3 minutes and bone wax used to seal the hole. The incision was then closed with surgical glue. The coordinates for stereotactic implantation were chosen based on pilot studies to result in generating a laterally positioned tumor within the cerebral hemisphere while avoiding injury to the thalamus and avoiding the seeding of the cerebrospinal fluid with tumor cells that may give rise to undesirable spinal tumors or ulcerating tumors into the orbit. To create PDOX using GBM-PDOs, a similar protocol was used with a few differences. GBM-PDOs were first dissociated into a single cell suspension using a protocol initially developed for primary bone marrow cells (Kokorina et al., 2012) and modified using the manufacturer's protocol (BD Cell Recovery Solution, #354253). The cells were then resuspended at 30,000 cells in 3  $\mu$ L media. These cells were then orthotopically injected at a rate of 0.5  $\mu$ L/minute. These mice were monitored until they reached 3 months post-injection, at which point MRI was performed, demonstrating GBM tumor formation. Mouse brains were collected for histological assessment of PDOX tumor formation with H&E and IHC staining.

### **Effects of 4D printed culture inserts on cell viability**

To determine how the culture inserts affected cell growth, cells were plated in the presence of varying concentrations of each of the individual components. Cells used included PDSs, PDOs, and U87MG cells. U87MG cells were grown in MEM (Gibco, REF #11090-081) with 1% pen/strep (Gibco, REF #15140-122) and 10% FBS (Sigma, F4135-500ML). Calculations for the concentrations were determined using the % volume of each component used in the inserts. A 10% of that was used to account for potential leaching effects. Cells were plated at 1,000 cells/condition. Cell viability was measured using the Promega Cell Titer Glo assay (Promega, REF #G7572). Cell viability was also assessed after plating with different sizes of the insert material and 4D printed culture insert material soaked for 5 days in acetone.

We first established optimum seeding densities for 3D cultures by determining the clonal efficiencies of deriving 3D cultures from dissociated patient cells at limiting dilutions to single cells

(Bansal et al., 2014; Vinci et al., 2012) to test the cell-culture insert arrays. Following seeding in the 4D printed culture inserts, GBM-PDOs were allowed to grow for 2 weeks. After 2 weeks, the media was aspirated from each well and replaced with media containing the treatment drug. Growth inhibitory conc. at 50% ( $GI_{50}$ ) conc. were determined for each drug, compared to untreated and DMSO-treated organoid cells. Temozolomide (TMZ) (Sigma, T2577) was used at a  $GI_{50}$  at 100  $\mu$ M, BEZ-235 (Selleck, S1009) at 1  $\mu$ M, and Niraparib (Selleck, S7625) at 4 nM. Cells were incubated at 37°C for 72 hours. Synergy screens consisted of dose response matrices ranging from 1X to 0.1X of the  $GI_{50}$  conc. for each drug. Isobologram for calculation and visualization of synergy scores from reduced GBM cell proliferation measured by ATP levels and synergistic response of the Bliss score surface observed using the combination of TMZ plus BEZ235 or niraparib plus BEZ235 were generated using the SynergyFinder application (Ianevski et al., 2017).

#### **Manual and automated histological processing of the 4D printed culture inserts**

After drug treatments, culture inserts were fixed in a dish containing PFA for 2 hours at RT. The dish was then moved to 50°C for 20 minutes to allow the cell-culture inserts to shrink. Inserts were then placed inside a cassette and taken to pathology for processing. Briefly, Cell-culture insert arrays underwent dehydration followed by embedding in a paraffin block. These blocks were then cut in 5  $\mu$ m sections using a microtome.

#### **Statistical analyses**

Data were normalized to the standard (Control). Analysis of significance was performed by two-way ANOVA with Bonferroni post-hoc test for comparing treatment effects and by Student's *t*-test when only two groups were compared using GraphPad Prism 8. Unless otherwise indicated, all experiments were performed at least thrice; *n* refers to biological replicates.

## SUPPLEMENTAL REFERENCES:

Ashammakhi, N., Ahadian, S., Zengjie, F., Suthiwanich, K., Lorestani, F., Orive, G., Ostrovidov, S., and Khademhosseini, A. (2018). Advances and Future Perspectives in 4D Bioprinting. *Biotechnol J* 13, e1800148.

Baeza, N., Weller, M., Yonekawa, Y., Kleihues, P., and Ohgaki, H. (2003). PTEN methylation and expression in glioblastomas. *Acta neuropathologica* 106, 479-485.

Bansal, N., Davis, S., Tereshchenko, I., Budak-Alpdogan, T., Zhong, H., Stein, M.N., Kim, I.Y., Dipaola, R.S., Bertino, J.R., and Sabaawy, H.E. (2014). Enrichment of human prostate cancer cells with tumor initiating properties in mouse and zebrafish xenografts by differential adhesion. *Prostate* 74, 187-200.

Kokorina, N.A., Granier, C.J., Zakharkin, S.O., Davis, S., Rabson, A.B., and Sabaawy, H.E. (2012). PDCD2 knockdown inhibits erythroid but not megakaryocytic lineage differentiation of human hematopoietic stem/progenitor cells. *Exp Hematol* 40, 1028-1042 e1023.

Kramer, J., Granier, C.J., Davis, S., Pisoni, K., Hand, J., Rabson, A.B., and Sabaawy, H.E. (2013). PDCD2 controls hematopoietic stem cell differentiation during development. *Stem Cells Dev* 22, 58-72.

Patel, N., Klassert, T.E., Greco, S.J., Patel, S.A., Munoz, J.L., Reddy, B.Y., Bryan, M., Campbell, N., Kokorina, N., Sabaawy, H.E., et al. (2012). Developmental regulation of TAC1 in peptidergic-induced human mesenchymal stem cells: implication for spinal cord injury in zebrafish. *Stem Cells Dev* 21, 308-320.

Vinci, M., Gowan, S., Boxall, F., Patterson, L., Zimmermann, M., Court, W., Lomas, C., Mendiola, M., Hardisson, D., and Eccles, S.A. (2012). Advances in establishment and analysis of three-dimensional tumor spheroid-based functional assays for target validation and drug evaluation. *BMC Biol* 10, 29.